



Measurement Techniques

Allan Howard,* Aston Chipanshi, Andrew Davidson, Raymond Desjardins, Andrii Kolotii, Nataliia Kussul, Heather McNairn, Sergii Skakun, and Andrii Shelestov

Abstract

Measurement techniques as they apply to agroclimate look beyond conventional instrumentation and methodologies, which are used to derive new data from direct observations of specific agrometeorological variables. They address the integration of the meteorological, hydrologic and biophysical variables critical for understanding the processes governing agricultural production and the agricultural interaction with the environment. Agroclimate measurement techniques also consider the temporal and spatial scales relevant to agriculture.

Soil moisture is a key variable for crop productivity, crop management practices, flood and excess moisture risk, and can control greenhouse gas emissions from farming operations. Crop condition and drought monitoring practices have been used as early warning for production and food security issues. Greenhouse gas flux is a critical indicator of the degree to which agriculture is either a source or a sink for greenhouse gases. Within each of these areas are multiple state of the art operational or near-operational techniques for measurement of indices and elements that pertain to spatial and temporal scales that are important for agriculture.

In an era of rapidly increasing availability of data, there are opportunities to better describe and measure the complexities of interactions influencing agricultural productivity and

Abbreviations: AVHRR, Advanced Very High Resolution Radiometer; CAR, Crop Census Agricultural Regions; ϵ , Soil dielectric permittivity; EO, Earth Observation; ESI, Evaporative Stress Index; ESU, Elementary Sampling Unit; FAPAR, fraction of absorbed photosynthetically active radiation; FCOVER, fraction of vegetation cover; FDR, Frequency Domain Reflectometry; GHG, greenhouse gases; GRACE, Gravity Recovery and Climate Experiment; ICCYF, Integrated Canadian Crop Yield Forecaster; IEM, integral equation model; LAI, Leaf Area Index; LUT, Look Up Table; MODIS, Moderate resolution Imaging Spectroradiometer; NDVI, Normalized Difference Vegetation Index; RCI, Rapid Change Index; SAR, synthetic aperture radar; SMAP, L-band Soil Moisture Active Passive; SPI, Standardized Precipitation Index; TDR, Time Domain Reflectometry; T_b , Brightness Temperature; VegDRI, Vegetation Drought Response Index; VI, Vegetation Indices; VWC, Vegetation Water Content; s_{θ} , backscatter; t , optical depth. A. Howard and A. Chipanshi, Agriculture and Agri-Food Canada, Science and Technology Branch, Regina, SK, Canada; A. Davison, R. Desjardins, and Heather McNairn, Agriculture and Agri-Food Canada, Science and Technology Branch, Ottawa, ON, Canada; A. Kolotii and A. Shelestov, National University of Life and Environmental Sciences of Ukraine, Kyiv, Ukraine; A. Kolotii, N. Kussul, S. Skakun, and A. Shelestov, Space Research Institute National Academy of Sciences and State Space Agency of Ukraine, Kyiv, Ukraine; A. Kolotii, N. Kussul, and A. Shelestov, National Technical University of Ukraine, Kyiv Polytechnic Institute, Kyiv, Ukraine. Received 7 Jan. 2016. Accepted 7 Jan. 2016. *Corresponding author (allan.howard@agr.gc.ca)

doi:10.2134/agronmonogr60.2014.0056.5

© ASA, CSSA, and SSSA, 5585 Guilford Road, Madison, WI 53711, USA.
Agroclimatology: Linking Agriculture to Climate, Agronomy Monograph 60.
Jerry L. Hatfield, Mannava V.K. Sivakumar, John H. Prueger, editors.

the agrienvironmental footprint. Measurement techniques are increasingly relying on sophisticated modeling and analysis techniques that integrate data from several sources to derive new information at the temporal and spatial scales required to support the agriculture sector's needs for science-based early warning and decision support.

Measurement of agrometeorological variables has been comprehensively covered (Hatfield and Baker, 2005; World Meteorological Organization, 2008; Petropoulos, 2014). These books cover standard operational procedures and equipment, siting and data recording. Agroclimatology focuses on the interaction of atmospheric, soil and biological factors that influence production of agricultural commodities and the environmental footprint associated with agricultural production. Measurement techniques for agroclimate must consider the integration of those meteorological, hydrologic and biophysical variables that are critical for agricultural production and the agricultural interaction with the environment, and do so at temporal and spatial scales relevant to agriculture.

The purpose of this chapter is to identify key state of the art operational or near-operational techniques and discuss them at scales that are relevant to agricultural production. The chapter focuses on three main types of techniques that are critical for determination of agricultural productivity and the agri-environmental footprint. Soil moisture is a key variable for crop productivity, crop management practices, flood and excess moisture risk, and is a controlling factor in greenhouse gas emissions from farming operations. Crop condition and drought monitoring techniques have been used as early warning for production and food security issues. Greenhouse gas flux is a critical indicator of the degree to which agriculture is either a source or a sink for greenhouse gases. This has implications for the sustainability of agriculture. Discussion is supported with case studies that apply the concepts and techniques toward measurement of each of these elements.

Soil Moisture

Soil moisture is a critical variable for several agrienvironmental and agricultural productivity factors. Stored moisture in the soil is a direct supply of water to the crop, and supplements growing season precipitation. It impacts latent heat fluxes that control the crop microclimate. It controls several biochemical processes related to pests, disease, rootzone oxygen exchange and fertility and is a controlling factor in runoff and groundwater recharge. In drier areas, where potential evapotranspiration exceeds precipitation, knowledge of spring soil moisture is a key element in determining several management practices, such as rates of fertilizer application, crop seeding rate and in some cases, crop selection. It is a key factor in assessment of drought risk and for establishing boundary conditions in weather forecast modeling.

Soil moisture is highly dependent on soil properties, landscape conditions, precipitation variability, land cover and freeze-thaw conditions. Consequently, soil moisture is highly spatially variable in most agricultural fields and cost effective means for determining soil moisture at field scales and depths relevant to agriculture remains a challenge.

This section covers soil moisture measurement techniques that are available over a range of scales. Typically in situ measurements offer the greatest spatial precision as they can be taken from direct contact with the soil and sampling or instrumentation can be placed at specified depths. However the main limitation of in situ measurement is that the pixel size for a measurement is typically a volume of a few cubic centimeters and therefore they are difficult to extrapolate to

field scale without extensive replication and cost. A limited number of intermediate scale surface observation techniques are available that offer the potential to assist in scaling up to field scale. Data from remote sensing techniques are relatively inexpensive and available at time intervals suitable for monitoring, but are available at scales coarse enough that a pixel represents several square kilometers.

In Situ Measurements

A wide variety of nondestructive or minimally destructive techniques have been developed over the past forty years that can be considered for use. Most are well-adapted to multiple measurements and/or monitoring of soil moisture at one location over a period of several seasons. All come with a variety of strengths and limitations.

Recent comprehensive reviews of soil moisture measurement techniques (Robinson et al., 2008; Dobriyal et al., 2012; Romano, 2014) show that there is no preferred method for determination of in situ soil moisture and that sensor technology is continually developing. A summary of some common techniques is presented in Table 1.

Electromagnetic techniques offer the most promising means of measurement of soil moisture because this category contains a range of techniques that measure the same soil water content proxy, the bulk soil dielectric permittivity (E), at scales ranging from localized in situ sensors, to intermediate (field) scale and remote sensing techniques (Huisman et al., 2003). In situ sensors in this category are typically well-suited to wireless observation networks where automated observations can be taken at temporal resolutions as fine as is required (e.g., from one measurement every several hours to measurements at subminute frequencies) for almost any application.

As the dielectric permittivity of water in the liquid phase ($E \sim 80$) is considerably larger than that of the soil matrix ($E \sim 4$ to 5) and air ($E \sim 1$), soil moisture has a dominant influence on soil dielectric permittivity. The soil permittivity is strongly determined by the content of water in the liquid phase in the soil. Because the dielectric permittivity of water in the frozen state drops to values comparable to the soil matrix, freezing and thawing of soil water can be determined by the appearance of a sudden “drying” of the soil when frozen and a sudden spike in the apparent water content during thawing.

The relationship between dielectric permittivity and soil is complex. When subjected to an alternating electrical field, preferred molecular alignment of the water molecules in the soil to that field requires the application of sufficient energy to overcome the random movement from thermal motion. The alignment process stores electrical energy, which becomes evident as dielectric permittivity. Dielectric permittivity is composed of two parts: (i) the real permittivity, or that stored energy that overcomes the random movement of the molecules, and (ii) the imaginary permittivity, or the influence of the ionic makeup of the soil solution that acts to dissipate the stored energy. The imaginary permittivity is referred to as dielectric loss (Robinson et al., 2003).

Dielectric loss can be attributed to two main processes: (i) electrical conduction and (ii) molecular relaxation (Robinson et al., 2003). Soil properties that enhance electrical conduction include salinity and exchangeable cations, whereas properties that influence molecular relaxation of the soil water are often associated with strong interactions between the soil surface and the solution (Seyfried et al., 2005). Dielectric loss can greatly complicate the calibration of sensors that use electromagnetic principles. A more detailed explanation of the relationship

Table 1. A summary of some common in-situ soil moisture measurement techniques.

Method	Mechanism	Strengths	Limitations
Acoustic Wave Oscillation (Meisami-asl et al., 2012)	Some properties of sound waves, including sweep frequencies (10 to 300MHz) and multiple tone sound have been correlated to soil moisture.	Less influence from soil properties and the potential for sampling larger volumes of soil that most sensors.	Still in an experimental stage.
Capacitance Sensors (Bogena et al., 2007; Dean et al., 1987)	Bulk permittivity of the soil is measured by an oscillating current. The magnitude of the resonant frequency is a function of soil moisture content.	Several types available. Geometry of sensors is adaptable for boreholes. Some are low cost; most require low maintenance.	Specific calibration of the soil is required. Susceptible to interference by bulk electrical conductivity and temperature.
Electrical Conductivity (EC) Sensors (Stenitzer, 1993)	EC of the soil solution is calibrated to soil moisture. Porous median such as gypsum blocks are placed in contact with the soil.	Suitable for continuous monitoring. Soil matric potential measured.	Does not measure volumetric soil moisture. Effective only in the wetter ranges of soil moisture.
Frequency Domain Reflectometry (Robock et al., 2000)	Bulk permittivity measured by reflected electromagnetic pulse reaching a set voltage (operate at 0.10 to 0.25 GHz)	Similar to Time Domain Reflectometry but with lower frequency and faster response time	Influence of clay dispersion on permittivity therefore unique soil calibration required. Well suited to remote automated data collection.
Gravimetric measurement (Gardner, 1965)	A soil sample is removed from the ground weighed in the moist state and then dried at 105°C to a constant weight.	Long history of use. It enables the determination of soil properties within the landscape when sampling for moisture.	The soil is disturbed. It is labor intensive and not well suited to monitoring. The soil bulk density is required to establish volumetric moisture content.
Ground Penetrating Radar (Huisman et al., 2002, 2003; Tran et al., 2015)	Bulk permittivity of the soil is measured using high frequency electromagnetic waves.	Suitable for use at field scales by moving the equipment across the soil using a sled or ATV taking multiple measurements.	Signals are complex to interpret, and complicated by surface roughness, salinity and variations in soil stratigraphy.
Neutron Moisture Meter (Chanasyk and Naeth, 1996)	Release a pulse of fast neutrons and count slow (thermalized) returned neutrons that become thermalized when in contact with hydrogen atoms	Reliable technology with a long history of use. Suitable for deep boreholes for monitoring deep rooted crops (e.g. alfalfa)	Requires use of radioactive materials that are restricted and require licensing. Not well-suited to automated data collection.
Tensiometers (Schmugge et al., 1980)	Measure soil water tension through negative pressure on water filled tube.	Direct measurement of soil matric potential	Volumetric soil moisture not measured, useful only in the wetter ranges of soil moisture.
Thermal Dispersion (Matile et al., 2013)	Release a pulse of heat and measure change in temperature in surrounding soil, with heat transmission closely related moisture	Alternative to electromagnetic methods	Sensitive to significant fraction of organic matter or coarse gravel
Time Domain Reflectometry (Topp et al., 1980)	Bulk permittivity of the soil is measured by time for EM pulse (frequency > 0.5 GHz) to travel along buried waveguide	Nondestructive and accurate. Less susceptible to interference by bulk electrical conductivity	Soils with high cation exchange capacity and organic soils require specific calibration.

between soil properties, frequency and dielectric permittivity can be found in Robinson et al. (2003), Seyfried et al. (2005) and Chen and Or (2006).

Sensors using dielectric properties to estimate soil moisture content in situ are typically in the form of probes that can be installed directly into the soil. They have been generally referred to as impedance probes (Cosh, 2005; Ojo et al., 2015). These probes measure the response of electromagnetic waves propagated along a coaxial cable to the bulk soil dielectric permittivity. Each probe has a set of parallel rods that are inserted in an undisturbed soil. The soil water acts as a resistance (impedance) that reflects the wave or a portion of it back to the source. These systems of measurement are nondestructive, suited to automated measurement and data collection, and accurate to within $\pm 1\%$ when the soil water is in the liquid phase over the range of field moisture conditions; although, measurements during the frozen state are not accurate without a specific calibration for that purpose.

There are two main methods of measuring the wave response. Time domain reflectometry (TDR) is based on the relationship between the travel time of the wave and the length of the rods in the sensor (Topp et al., 1980). Frequency domain reflectometry (FDR) probes use variations in the frequency of the signal resulting from the soil permittivity to estimate soil moisture content (Dobriyal et al., 2012). The higher frequencies of the TDR reduce the sensitivity of the response to soils properties such as salinity, texture or temperature (Robinson et al., 2008). FDR probes operate at lower frequencies (e.g., 50 to 150 MHz compared to over 1000 MHz for TDR probes) and are therefore more susceptible to influence from these soil properties. Some FDR probe models come with hardware and software to independently measure temperature and electrical conductivity, thus enabling them to more accurately determine the influence from soil properties and salinity, which comprise the dielectric loss or imaginary permittivity component.

Frequency domain reflectometry-type probes are popular because of their lower cost, in terms of both capital investment and time. Their lower power consumption requirements coupled with the ability of the probes to be multiplexed with dataloggers make them attractive for remote monitoring.

Impedance probes are the standard soil moisture sensor for the Canadian Real-time In situ Soil Monitoring for Agriculture (RISMA) network (Adams et al., 2015), and the United States national cooperative network, the United States Department of Agriculture Natural Resources Conservation Service (USDA-NRCS), and Soil Climate Analysis Network (SCAN) (Schafer et al., 2007). The publicly available data from these networks contain surface meteorological and soil moisture data at hourly resolution. Data from SCAN were correlated with (i) satellite-based active and passive microwave signatures in an agricultural landscape (Nghiem et al., 2012), (ii) in validation of the Variable Infiltration Capacity (VIC), Decision Support System for Agrotechnology Transfer (DSSAT), and Climatic Water Budget (CWB) models (Meng and Quiring, 2008) and (iii) in validation of drought indicators derived from water storage data from the Gravity Recovery and Climate Experiment (GRACE) satellites (Houborg et al., 2012). As explained below in "Drought Monitoring", the GRACE-derived drought indicators were particularly useful as proxy for the sparse availability of ground-based observations of soil moisture and groundwater for drought monitoring (Houborg et al., 2012).

Intermediate Scale Measurements

Cosmic Ray Techniques

Determination of field soil moisture by the use of sensors to detect the intensity of passive neutrons generated by the interaction of cosmic rays with terrestrial atoms has been discussed in Zreda et al. (2008). The ratio of high energy neutrons to low energy neutrons above the landscape surface is inversely correlated with the number of hydrogen (H) atoms in the soil and therefore can be related to area averaged soil moisture content. The method is relatively insensitive to variations in soil chemical properties, although sensitivity to variations in organic matter within the soil or to vegetative growth on the landscape merits consideration. The cosmic ray probe is mounted above the soil surface and measures the flux of high energy (fast) neutrons.

The Cosmic ray Soil Moisture Observing System (COSMOS) is a continental-scale network consisting of instruments designed to improve the availability of continental-scale soil moisture measurements by ultimately deploying a network of 500 cosmic ray probes across the United States (Zreda et al., 2012).

One potential source of uncertainty is the influence of the H content of biomass. The largest and most variable pool of H is from soil moisture. The H content of biomass is considered to be relatively constant however the contribution from variation in atmospheric humidity is significant enough that a correction factor is recommended (Zreda et al., 2012). Franz et al. (2013) was able to separate the contribution from soil moisture to estimate biomass water equivalent in a pine forest and in a maize field; however, they acknowledge that uncertainties arose from several factors including humidity and assumptions used in determining the forest component of the landscape. A dry bias in cosmic ray derived near-surface soil moisture data in a mixed forest following snowmelt has also been observed (Lv et al., 2014). Snowcover over 6 cm deep or the presence of surface water can make determination of soil moisture impossible (Zreda et al., 2012).

One significant feature of the cosmic ray method is that the sampling footprint at sea level can be 300 m in radius (Baatz et al., 2014). The sensitivity to thermalized neutrons attenuates with moisture content and depth, and the depth of measurement varies from 12 cm in wet soils to 70 cm in dry soils (Franz et al., 2013).

The cosmic ray techniques offer an opportunity to measure a broader footprint of soil moisture that is more representative of field scale, and therefore offers an intermediary scale between the point measurements of the previously mentioned techniques and the broader-scale remote sensing techniques.

Remote Sensing Measurements

Remote sensing measures the amount of radiation emitted, reflected and transmitted by a target. Sensors record this energy in one or more electromagnetic frequencies and through modeling the power of the detected energy can be related to a target parameter, such as soil moisture. The bulk soil permittivity (ϵ) can be detected by sensors when the land surface is subjected to applied electromagnetic fields at microwave frequencies (wavelengths of 1 to 100 cm). Soils with higher moisture have greater reflectivity, as the power of the energy reflected (and by reciprocity emitted) is related to the dielectric permittivity through the Fresnel equations (Ulaby et al., 1986).

For time-sensitive applications, microwave sensors have a distinct advantage over optical sensors operating at shorter visible-infrared wavelengths. At longer microwave wavelengths atmospheric contributions to emission and scattering are minimal, enabling the collection of data even in the presence of clouds and haze.

Microwave remote sensing can be applied either passively or actively, both with advantages and disadvantages. Tables 2 and 3 present passive and active satellites suitable for estimating soil moisture. Whether passive or active approaches are used, these sensors measure moisture in only the near surface volume (top few centimeters). The depth of sensing (penetration depth) is not set, but is dependent primarily on the frequency and incident angle of the sensor, and on the soil wetness. This

Table 2. Specifications of Selected Space-borne Passive Radiometers.

	Special Sensor Microwave/Imager (SSM/I)	Soil Moisture and Ocean Salinity (SMOS)	Advanced Microwave Scanning Radiometer 2 (AMSR-2)	Soil Moisture Active Passive (SMAP)
Country	United States	European Space Agency	Japan	United States
Launch Date	1987	2009	2012	2015
Frequencies (GHz)	19.3, 22.2, 37.0, and 85.5	1.4	6.9, 7.3, 10.6, 18.7, 23.8, 36.5, 89.0	1.4
Approximate Ground Resolution (km)	37 by 28 (37 GHz) 15 by 13 (85.5 GHz)	35 to 50	62 by 35 (6.9 GHz) 5 by 3 (89.0 GHz)	40
Swath (km)	1400	1000	1450	1000

Table 3. Specifications of Selected Space-borne Synthetic Aperture Radars.

	TerraSAR-X	RADARSAT-2	Radar Imaging Satellite (RISAT)	Advanced Land Observing Satellite 2 (ALOS-2) PALSAR	Sentinel-1
Country	Germany	Canada	India	Japan	European Space Agency
Launch Date	2007 2010 (TanDEM-X)	2007	2012	2014	2014
Band (wavelength-cm)	X (3.1)	C (5.6)	C (5.6)	L (22.9)	C (5.6)
Frequency (GHz)	9.7	5.4	5.35	1.2	5.4
Approximate Ground Resolution (m)	1 to 16	3 to 100	2 to 50	1 to 100	5 to 100
Nominal Swath Width (km)	1 to 100	10 to 500	10 to 240	25 to 490	20 to 400
Exact Repeat Cycle (days)	11	24	25	14	12

depth is a fraction of the incident wavelength and is estimated between one-tenth (modeled) to one-quarter (measured in the field) of a wavelength (Jackson, 2002).

Measurement by Passive Microwave Techniques

Passive radiometers detect microwave energy naturally emitted by the Earth. The magnitude of emitted energy at microwave frequencies is quite small and thus, radiometers must integrate over large footprints to record a strong enough signal relative to background and system noise (Jensen, 2007). Hence space-based radiometers have very coarse resolutions, on the order of tens of kilometers. Passive microwave satellites image very large swaths and thus provide soil moisture products at regional and national scales at relatively frequent temporal intervals (1–2 d at high latitudes and 3 d at the Equator) (Pacheco et al., 2015).

Passive radiometers record responses as brightness temperature (T_B). T_B is a function of the emissivity (ϵ) and physical temperature (T) of the soil ($T_B = \epsilon T$). Soils with higher moisture content have lower emissivity and accordingly, lower T_B . If present, vegetation attenuates soil emissions and contributes to its own microwave emissions, complicating soil moisture retrieval (Jackson, 2002). Attenuation is characterized by the optical depth (τ) which is empirically related to the vegetation water content (VWC); τ is vegetation-type specific (Elachi and van Zyl, 2006). Soil roughness also affects the T_B . Roughness increases surface area and emissivity. In almost all cases, approaches to retrieve soil moisture from T_B use an approximation of the radiative transfer equation known as the tau-omega (τ - w) model, where w is the single scattering albedo (Mladenova et al., 2014). In the absence of vegetation, estimating emissivity is easily accomplished using radiometer-measured T_B and a measure of temperature. When a canopy is present, τ must be estimated from a measure of VWC to adjust for attenuation effects. While T_B is provided by one radiometer polarization, measures of temperature, VWC and roughness are determined from ancillary sources (i.e., single channel approach where for example, VWC is estimated from the optically-derived Normalized Difference Vegetation Index) or from a second polarization on the same radiometer (dual channel approach) (Mladenova et al., 2014). Radiometers measure a large dynamic range in brightness temperature. At L-band (1.4 GHz) T_B decreases by ~ 70 K from dry to saturated soils (Elachi and van Zyl, 2006). Considering this sensitivity, T_B can be inverted to estimate soil moisture at accuracies of about 0.04 g cm^{-3} when vegetation present has a VWC less than 5 kg m^{-2} (Elachi and van Zyl, 2006).

Measurement by Active Microwave Techniques

In contrast, active microwave sensors (Synthetic Aperture Radars or SARs) generate their own energy, propagating pulses of microwaves and detecting the power of the energy scattered back to the sensor. Spatial resolutions of SARs are much finer, on the order of meters, relative to passive sensors. However, the width of swaths imaged by SARs is much smaller and therefore more overpasses are required to provide the same spatial coverage as passive sensors. With a smaller swath, a SAR satellite re-images a specific area less frequently. Constellations (such as the proposed RADARSAT Constellation) are needed to achieve an equivalent temporal frequency and spatial coverage as that of passive systems.

Active sensors measure the power of energy scattered back to the sensor (backscatter (s°)) proportionate to the power propagated by the radar. This two-way transmission results in complex scattering and a more challenging soil

moisture retrieval. Backscatter is highly sensitive to the incident angle of the transmitted wave and polarization of the transmitted and received wave. The geometry (soil and vegetation) affects scattering behavior (single, double or multiple scattering), while dielectric properties affect the scattering power (Dobson and Ulaby, 1998). Both higher soil moisture content and rougher soils lead to greater scattering. As such, retrieval approaches must model both dielectric and roughness contributions to s^o . The Integral Equation Model (IEM) is physically based and integrates the small perturbation, geometric and physical optics models (Fung and Chen, 1992). The IEM is appropriate for a wide range of moisture and roughness conditions. Inversion of the model is complex and thus Look Up Table (LUT) approaches have been used, yielding soil moisture errors of about 0.04 g cm^{-3} when two incident angles and polarizations are exploited (Merzouki and McNairn, 2015). Semi-empirical models such as the Oh model and the Dubois model simplify the scattering problem, primarily by reducing roughness parameters (Oh et al., 1992; Dubois et al., 1995). Accuracies with these models, for non-vegetated soils, are reported in the range of 0.04 g cm^{-3} (Dubois model) and 0.08 g cm^{-3} (Oh model) (Merzouki et al., 2011). Vegetation creates multiple two-way scattering, greatly complicating soil moisture retrieval. The semi-empirical Water Cloud Model (WCM) represents the backscatter power as the incoherent sum of contributions from vegetation (s^o_{veg}) and soil (s^o_{soil}) (Attema and Ulaby, 1978). However using C-band data and the WCM, Jiao et al. (2011) found limited sensitivity to soil moisture under established canopies. L-band microwaves penetrate deeper into the canopy. The L-band Soil Moisture Active Passive (SMAP) satellite will estimate soil moisture under vegetation by inverting 3-dimensional crop specific LUTs of complex forward radar models. Prelaunch validation using L-band airborne data yielded retrieval accuracies from 0.037 to 0.086 g m^{-3} depending on crop type (McNairn et al., 2015).

Crop Condition and Drought Monitoring

Crop condition monitoring refers to repeated measurement and reporting of the changing growth and development aspects of crops and pastures during the growing season. Regional and national scale crop monitoring and reporting are increasingly based on satellite based optical sensors such as the Moderate resolution Imaging Spectroradiometer (MODIS). Optical sensors have an advantage over microwave sensors for crop condition applications by sensing those wavelengths reflected as a result of plant biophysical processes. However these wavelengths are obscured by cloud cover, limiting the time available for measurement. MODIS data at the 250-meter resolution is supported by weather data obtained from land-based climate stations or satellite platforms. A reporting time frame such as weekly or biweekly is chosen to assess growth and development elements.

Apart from providing vital scientific data on plant growth and development, crop condition monitoring is driven by (i) the increasing societal awareness and the need to know the adverse impacts of the environment on the food production systems, (ii) information demand from producers, grain traders, and government policymakers as well the agricultural industry as a whole to assist their decision making, and (iii) concerns about the future global food insecurity and the attendant social problems. The proliferation of satellite based sensors with global coverage has made data suitable for crop condition assessment data widely

Table 4. Examples of crop condition monitoring activities and products.

Country	Agency	Product	More information
Australia	Australian Bureau of Agricultural and Resource Economics and Science (ABARES)	National commodity forecasts	
	Queensland Alliance for Agriculture and Food Innovation (QAAFI), and Department of Agriculture and Food of Western Australia (DAFWA)	State and shire commodity forecasts	Nikolova et al. (2012)
Canada	Statistics Canada	Crop Condition Assessment Program (CCAP)	Reichert and Caissy (2002)
	Agriculture and Agri-Food Canada	Canadian Crop Yield Forecaster	Chipanshi et al. (2012)
China	Institute of Remote Sensing and Digital Earth (RADI) at the Chinese Academy of Sciences	China Crop Watch	Wu et al. (2014)
Europe	Joint Research Centre (JRC) of European Commission	Monitoring Agriculture with Remote Sensing (MARS) Crop Yield Forecasting System	Joint Research Centre (2012)
United States	US Department of Agriculture National Agricultural Statistics Service (NASS)	Cropscape	Han et al. (2012)
	NASS in collaboration with the Joint Agricultural Weather Facility (JAWF) of USDA and NOAA	World Agricultural Supply and Demand Estimates Report (WASDE)	USDA (2012)
Global	U.S. Agency for International Development (USAID)	Famine Early Warning Systems Network (FEWS)	http://www.fews.net
	United Nations Food and Agriculture Organization (FAO)	Global Information and Early Warning System (GIEWS)	http://www.fao.org/giews
	Group on Earth Observation (GEO)	GEO Global Agricultural Monitoring (GEOGLAM)	http://geoglam-crop-monitor.org/
	GEO Joint Experiment on Crop Assessment and Monitoring (JECAM)	JECAM Annual Progress Report	http://www.jecam.org

available at frequencies and resolutions suitable for crop monitoring, inexpensive and reliable. As a result, many countries have developed crop monitoring systems from satellite-based data supported by ground-based data, or collectively Earth Observation (EO) data. Examples of such systems are presented in Table 4.

Vegetation Indices

Remotely-sensed data collection has the potential to provide quantitative information on the amount, condition, and type of vegetation, provided that the effects of physical and physiological processes on the spectral characteristics of canopies are fully understood.

One of the greatest challenges in the remote sensing of agricultural systems has been the reliable estimation of biophysical variables (such as aboveground biomass, net primary productivity and yield) from satellite platforms. This is largely a consequence of the “mixed pixel” problem, where factors other than the presence and amount of green vegetation (e.g., senescent vegetation, soil, shadow)

combine to form composite spectra (Asner, 1998; Asner et al., 1998; Fourty et al., 1996; Goel, 1988; Myeni et al., 1989; Ross, 1981). Spectral mixing often makes the discrimination of green vegetation difficult and has prompted the development of numerous spectral vegetation indices (VIs). VIs are dimensionless radiometric measures that combine two or more spectral bands to enhance the vegetative signal, while simultaneously minimizing background effects. Vegetation indices are one of the most widely used remote sensing measurements, and thus, many exist. The most common VIs utilize red (*R*) green (*G*) blue (*B*), near-infrared (NIR) and/or shortwave infrared (SWIR) canopy reflectance. The indices are described in Table 5. Although many indices are well correlated with various plant biophysical parameters some, such as the Normalized Difference Vegetation Index, have received more attention than others.

The Normalized Difference Vegetation Index (NDVI) can be calculated from the red and near infrared data acquired by several satellite systems (Table 5). The principle behind the NDVI is based on the relationship between the physiological properties of healthy vegetation and the type and amount of radiation it can absorb and reflect (Gitelson and Kaufman 1998). More specifically, plant chlorophyll strongly absorbs solar radiation in the red portion of the electromagnetic spectrum, while plant spongy mesophyll strongly reflects solar radiation in the near-infrared region of the spectrum (Jackson and Ezra 1985; Tucker 1979; Tucker et al., 1991). As a result, vigorously growing healthy vegetation has low red-light reflectance and high near-infrared reflectance, and hence, high NDVI values.

The NDVI produces output values in the range of -1.0 to 1.0. Increasing positive NDVI values indicate increasing amounts of green vegetation, while NDVI values near zero and decreasing negative values are characteristic of non-vegetated surfaces such as barren surfaces (rock and soil) and water, snow, ice, and clouds (Jensen 2007). It is important to note, however, that because the NDVI becomes less sensitive to plant chlorophyll at high chlorophyll contents, the NDVI approaches saturation asymptotically under moderate-to-high biomass conditions (Baret and Guyot 1991; Gitelson and Kaufman 1998; Huete et al., 2002; Myneni et al., 2002; Sellers 1985). As a result, although the NDVI has been shown to correlate well with many canopy biophysical properties, including vegetation abundance (Hurcom and Harrison 1998; Purevdorj et al., 1998), aboveground biomass (Boutton et al., 1980; Davidson and Csillag 2001; Weiser et al., 1986), green leaf area (Asrar et al., 1986; Baret and Guyot 1991; Weiser et al., 1986), photosynthetically active radiation (PAR) (Asrar et al., 1986; Baret and Guyot 1991; Hatfield et al., 1984; Tucker et al., 1986; Weiser et al., 1986), and productivity (Box et al., 1989; Prince 1991; Running et al., 1989), it generally does so in a nonlinear fashion across low-to-high productivity gradients.

The NDVI has emerged as one of the most robust tools for monitoring natural vegetation and crop conditions. The most commonly-used products are n-day (e.g., 7 or 10 d) maximum-value NDVI (Max-NDVI) composites and their associated anomalies (the associated NDVI differences from "normal conditions") (Cracknell 2001). While the detailed methodologies for creating these datasets vary, maximum-value compositing usually involves (i) examining each NDVI value pixel by pixel for each observation date during the n-day compositing period, (ii) determining the maximum-value NDVI for each pixel during the n-day period, and (iii) creating a single-output image that contains only the maximum NDVI value for each pixel for the n-day period. Maximum-value NDVI compositing has become a popular resource management tool because it captures the dynamics of green

vegetation and minimizes problems common to single-date NDVI data, such as those associated with interference from cloud cover, atmospheric attenuation, surface directional reflectance, and view and illumination geometry (Holben, 1986).

The Advanced Very High Resolution Radiometer (AVHRR) instruments that have been flown onboard 14 of NOAA's Polar Orbiting Satellites since 1978 have been considered the longest-lived and most influential series of Earth-observing satellites ever launched (Hastings and Emery, 1992). Since some VIs that have been applied, including NDVI, are based on anomalies during the period of record for observations, the long data record of AVHRR data has been particularly useful. The AVHRR, originally designed for meteorological applications, senses in the visible, near-infrared, and thermal infrared portions of the electromagnetic spectrum at a spatial resolution of 1.1 km. However, because the AVHRR sensor was not originally designed for monitoring vegetation, it suffers from limitations regarding the design of its red and near infrared channels when formulating NDVI (Fensholt and Sandholt, 2005). Two particularly important limitations of the AVHRR are (i) the overlap of the near infrared channel (0.725 to 1.100 μm) with a region of considerable atmospheric water vapor absorption (0.9 to 0.98 μm) that can introduce noise to the remotely sensed signal (Huete et al., 2002; Justice et al., 1991); and (ii) the relatively "quick" saturation of the red channel, and hence VIs derived from it, over medium-to-dense vegetation (Gitelson and Kaufman, 1998; Huete, 1988; Jensen, 2007; Myneni et al., 1997).

These limitations were directly addressed with the development of a new generation of EO platforms including the moderate resolution imaging spectroradiometer (MODIS) launched onboard NASA's Terra satellite in Dec. 1999. MODIS, which has been acquiring data in 36 narrow spectral bands since Feb. 2000, was designed to provide data for vegetation and land cover mapping applications. The MODIS sensor offers a number of improvements over the AVHRR for NDVI calculation (Fensholt and Sandholt, 2005; Huete et al., 2002; Trishchenko et al., 2002). These include improved (i) spectral resolution, (ii) radiometric resolution, (iii) spatial resolution, (iv) geolocation accuracy, and (v) on-board radiometric calibration for producing scaled reflectances (Jensen, 2007). The MODIS red and near-infrared channels were selected to avoid the spectral regions of water absorption that constitute a major limitation of the AVHRR (Justice et al., 1991; Vermote and Saleous, 2006). Furthermore, the unprecedented radiometric resolution of MODIS-Terra makes its red and near-infrared channels more sensitive to small variations in chlorophyll content, thereby lessening how quickly its NDVI saturates over denser vegetation. As a result of these improvements, MODIS-Terra holds promise for environmental monitoring in general and the estimation of vegetation indices in particular (Fensholt and Sandholt, 2005).

Yield Estimation and Forecasting

Traditionally, regional or national crop yield estimates were made by field or farmer surveys conducted during or after the crop growing season (e.g., USDA, 2012; Statistics Canada, 2012). The survey method was resource intensive and significant time lags in data processing meant that reliable estimates were not normally available until long after the growing season. For example, Statistics Canada conducted national crop yield surveys in July, September and November and the last (or the most reliable) yield estimates were released in early December while most crops were harvested 2 to 3 mo earlier. To reduce the costs associated

with surveys and to increase the lead time of the crop yield estimates, tremendous efforts have been made by several countries to incorporate EO-based VI methods for in season crop monitoring which provide the capability of producing crop yield forecasts (e.g., Potgieter et al., 2006; de Wit and van Diepen, 2007; Semenov and Doblas-Reyes, 2007; Qian et al., 2009; Mkhabela et al., 2011; Bornn and Zidek, 2012; Chipanshi et al., 2012; Nikolova et al., 2012).

In Canada the Integrated Canadian Crop Yield Forecaster (ICCYF), a statistical yield forecasting tool integrates remote sensing and agroclimate data in near real time to forecast grain and oil seed crops with a lead time of 2 to 3 mo starting in July (Newlands et al., 2014; Chipanshi et al., 2015). The ICCYF was first calibrated using NDVI as derived from the AVHRR sensor at 1 km resolution, combined with the corresponding agroclimatic indices from ground-based climate stations (e.g., water stress, accumulated precipitation and growing degree days) against regional crop yield as reported by Statistics Canada from 1987 to 2012. The basic unit for comparison was the Crop Census Agricultural Regions (CARs), units of approximately 1000 km². The calibrated model from each CAR uses the near real time NDVI and climatic indices from seeding to the prediction date as model inputs. Beyond the prediction date to the end of the season, the unobserved variables that are required to make a forecast are estimated from a statistical procedure called random forest (Liaw and Wiener, 2002). The use of the random forest scheme takes advantage of the posterior statistical distribution of the predictor variables which is generated from the Markov-chain Monte Carlo algorithm (Dowd, 2006). Since outlook projections of crop yields from EO data started in 2013, the ICCYF has consistently generated yield results that are not statistically different at the CAR level from the final observed yield numbers that are released in November by Statistics Canada. Due to the similarity between official numbers and ICCYF simulations and the gain in lead time by the ICCYF over the survey methods, there have been discussions to replace some of the survey results with simulated values in the near future.

The skill in yield predictions with the ICCYF is expected to improve further when crop specific masks are used to generate NDVI values in near real time. Currently, a generalized agriculture crop mask is used for all crops. Changes to the ICCYF algorithms under extreme weather (when results are less reliable) are being tested.

Drought Monitoring

Measurement and monitoring of drought have challenges because the physical factors such as precipitation variability do not always predict the impacts of drought; the onset and recession of drought is imprecise and the spatial and temporal variability of drought can be large. The common factor in drought is that droughts develop from a deficiency of precipitation that results in water shortages for some activity or for some group (Wilhite and Glanz, 1985).

Quantification of drought severity was originally based on meteorological and/or hydrological data. Several indices have been developed and have been reviewed for use in the United States (Heim 2002, Keyantash and Dracup 2002) and globally (Vicente-Serrano et al., 2012). Some of the most commonly used indices include the (i) Palmer Drought Severity Index (Palmer, 1965) based on soil conditions and current and prior climatological conditions, (ii) the Surface Water Supply Index (Shafer and Dezman, 1982; Garen, 1993), based on non-exceedance probabilities of normalized data for snowpack, precipitation, streamflow and

reservoir storage, and (iii) the Standardized Precipitation Index (SPI) (McKee et al., 1993; World Meteorological Organization, 2012) based on the non-exceedance probabilities based on the normalized variance of regional precipitation over the period of record for a specified time period, such as monthly or yearly. The SPI does not include a temperature component and therefore ignores the contribution of temperature variability in drought severity, which could be a limitation in areas where potential evapotranspiration (PE) exceeds precipitation (P). The Standardized Precipitation and Evaporative Index (Vicente-Serrano et al., 2010) was developed with the incorporation of a P-PE component where PE can be calculated from temperature using established PE models such as the Penman-Monteith or Thornthwaite models, depending on availability of input data.

Recent increases in data handling and modeling techniques and the increasing availability of remote sensing data have resulted in development of indices that integrate meteorological and biophysical expressions in the landscape and allow satellite-based monitoring of drought conditions. The United States Drought Monitor (USDM) (Svoboda et al., 2002) uses a hybrid of meteorological and hydrological indices combined with remotely-sensed vegetation indices to provide a weekly national assessment of drought for the United States. It has been the model for other drought monitoring efforts such as the North American Drought Monitor (NADM) <https://www.ncdc.noaa.gov/temp-and-precip/drought/nadm/>.

The Vegetation Drought Response Index (VegDRI) (Brown et al., 2008) integrates traditional climate-based drought index information, SPI and PDSI, with satellite-based Normalized Difference Vegetation Index (NDVI). The VegDRI therefore assesses the effects of drought on vegetation by observing the vegetation conditions from satellite and the level of dryness from climate data. Brown et al. (2008) reported that more spatially-detailed drought information could be obtained using VegDRI than what was available with the USDM.

Anderson et al. (2007) used remotely sensed land surface temperature from thermal infrared imagery from the GOES satellite to derive temporal anomalies in the ratio of actual evapotranspiration (ET) to PE, which were expressed as the Evaporative Stress Index (ESI). The ESI provides anomalies in the values of the ratio of ET to PE compared to historic data. Patterns of water stress can be determined at a spatial resolution of 5 to 10 km over continental scales. The ESI compared favorably with drought conditions as determined by the USDM (Anderson et al., 2007) and it is currently used operationally. Its application to United States drought conditions can be observed at the National Oceanic and Atmospheric Administration's National Integrated Drought Information System website <https://www.drought.gov/drought/content/products-current-drought-and-monitoring-remote-sensing/evaporative-stress-index>.

Rapid onset of drought or "flash drought" conditions were observed in the Central Plains of the United States during the summer of 2012 (NOAA Drought Task Force, 2013). The combination of below normal rainfall, above normal temperatures, sunshine and wind greatly increase PE rates resulting in rapid drying conditions (Otkin et al., 2013). The Rapid Change Index (RCI) (Otkin et al., 2014) was developed to assess the cumulative magnitude of weekly ESI changes, which were correlated to the onset of drought conditions as determined by the USDM. During the 2012 drought they provided sensitivity to drought onset a month before the USDM drought assessment rapidly deteriorated from no drought to extreme drought. Otkin et al. (2015) applied the RCI to changes in evapotranspiration, precipitation and soil moisture to provide early warning of drought

across the continental United States, they noted that while proving the concept that rapid decline in the three indices can be used to identify areas susceptible to drought onset and intensification, further validation is required before it can be used with confidence for operational purposes.

Soil moisture and drought indicators have been generated from the NASA and GRACE satellites. These twin satellites are sensitive enough to detect small changes in the earth's gravitational field caused by water redistribution at or beneath the earth's surface. Total terrestrial water storage data from the GRACE system have a monthly temporal resolution, and a coarse (150, 000 km²) spatial resolution. To make the information useful for drought monitoring, the GRACE Data Assimilation System (Zaitchik et al., 2008) was used to integrate GRACE TWS data with meteorological observations from both ground observation stations and satellite based sensors. This enabled the downscaling and stratification of the TWS data into basin scale surface soil moisture, rootzone soil moisture and groundwater storage for the continental United States as near real time drought indices and compared with the United States and North American drought monitors. The data substituted for the sparse availability of ground-based observations of soil moisture and groundwater. The groundwater data in particular contributed a longer-term component to the anomalies associated with drought (Houborg et al., 2012). Operational weekly water storage data map products based on the hybridized GRACE data are available at the National Drought Mitigation Centre website <http://drought.unl.edu/MonitoringTools/NASAGRACEDataAssimilation.aspx>.

Case Study: Crop Condition Assessment in the Ukraine

Crop condition assessment is an important component of agriculture resource monitoring. Globally available products on crop condition assessment provide an extremely important input to food security within, for example, the Global Agriculture Monitoring (GLAM) initiative. In the Ukraine, such information allows for the identification of crop phenological indicators and could be used for prediction of both crop yield (Kogan et al., 2013) and crop production (Kussul et al., 2013; Kussul et al., 2014).

Leaf area index (LAI), fraction of absorbed photosynthetically active radiation (FAPAR) and fraction of vegetation cover (FCOVER) are indicators that characterize the crop state (Camacho et al., 2013). Coarse resolution images acquired by SPOT-VEGETATION, MODIS, and PROBA-V are used to provide regular and timely products on biophysical parameters at global scale. To provide consistent and reliable information these products should be validated using ground measurements. Hence, the particular objectives of this case study are: (i) to validate global biophysical products with use of in situ data, and (ii) to assess the efficiency (in terms of prediction error minimization) of satellite based data when assimilated into winter wheat crop yield forecasting models.

A study area in Onufriivka county of Kirovohrad region was selected for winter wheat forecasting. For the validation of the required biophysical parameters, a JECAM (Joint Experiment of Crop Assessment and Monitoring) test site was chosen. All surveys on the JECAM test site were conducted on two scales: local subsite (Pshenichne test site) of 3 by 3 km and a medium scale (county-level) site of approximately 1000 km² (Camacho et al., 2013).

Three field campaigns in 2013 (14 to 17 May, 12 to 15 June and 14 to 17 July) and two field campaigns in 2014 (12 June and 31 July) were conducted to characterize the

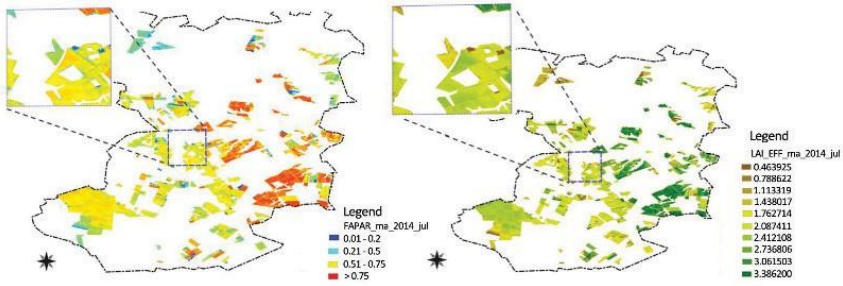


Fig. 1. Biophysical maps for maize, derived from Landsat-8, fraction of absorbed photosynthetically active radiation (FAPAR) as for 31 July, 2014 (left); Leaf Area Index (LAI) effective as for 31 July, 2014 (right).

vegetation biophysical parameters at the Pshenichne test site. Digital Hemispheric Photographic (DHP) images were acquired with a NIKON D70 camera by staff standing above the crop. Hemispherical photos allow the calculation of LAI and FCOVER by measuring gap fraction through an extreme wide-angle camera lens (i.e., 180°). The hemispherical images acquired during the field campaign are processed with the CAN-EYE software (http://www.avignon.inra.fr/can_eye) to derive LAI, FAPAR and FCOVER estimations. The in situ biophysical values are used for producing LAI, FCOVER and FAPAR maps from optical satellite images, and provide cross-validation, and validation of global remote sensing products (Morissette et al., 2006).

Satellite imagery acquired from Landsat-8 (at 30 m spatial resolution) was used to support ground observations and provide high-resolution biophysical maps. SPOT Vegetation products LAI and FAPAR (at 1 km resolution) used in this study for yield forecast model calibration were obtained from Copernicus Global Land Service (<http://land.copernicus.eu>).

Ground observations follow the Validation of Land European Remote sensing Instruments (VALERI) protocol in which the measurements are made for a set of elementary sampling units (ESUs) (Baret et al., 2005). The center of each ESU is georeferenced using a Global Positioning System device. A pseudoregular sampling grid is used within each ESU of approximately 20 by 20 m. The number of hemispherical photos per ESU ranges between 12 and 15. The number of ESUs varied from year to year depending on available resources. During the three 2013 campaigns 30, 34, and 37 ESUs were sampled whereas during the two campaigns in 2014, 28 and 25 ESUs were sampled.

The NDVI specific for winter wheat specific, with use of a dynamic crop mask (a mask developed every year) is used as the main variable to derive three biophysical values (LAI, FAPAR, FCOVER) from satellite images. Two types of models are considered to relate NDVI to each of the three biophysical parameters estimated from ground measurements: linear ($Y = b_0 + b_1 * NDVI$) and exponential ($Y = b_0 * \exp(b_1 * NDVI)$), where Y is either LAI, FAPAR or FCOVER and b_0 and b_1 are adjustable parameters of the regression model. The following metrics are used to assess efficiency of the models: (i) root mean square error (RMSE); (ii) cross-validation RMSE with a leave-one-out method (RC); (iii) model's adjusted coefficient of determination r^2 . Yield is estimated as a sum of the trend component and deviation from trend, caused by the current situation with vegetation development.

Deviation is estimated with a linear single-factor regression model (Kogan et al., 2013; Kussul et al., 2014; Camacho et al., 2013).

Relationships between satellite-derived NDVI values and ground measurements of biophysical parameters were developed using both linear and exponential models. The best results for winter wheat have been achieved with a single factor exponential model for LAI (up to $r^2 = 0.84$) and linear single factor models for FAPAR (up to $r^2 = 0.84$). Samples of created biophysical maps are shown in Fig. 1. These maps are used for validation of global LAI and FAPAR products derived from Copernicus Global Land Service.

Biophysical products (FAPAR and LAI) are more preferable to be used as predictors in crop yield forecasting regression models. Corresponding models possess much better statistical properties and are more reliable than the NDVI based model. The most accurate result in the study to date has been obtained for LAI values derived from SPOT-VGT (at 1 km resolution) on county scale averaged using the crop mask (with $r^2 = 0.86$).

Therefore, we have concluded that for the Ukraine, LAI and FAPAR are the best variables for developing accurate, reliable regression based models for winter wheat yield forecasting at the county level. Models calibrated with biophysical parameters are much more accurate than models calibrated with classical vegetation indices (NDVI) and global biophysical products agree sufficiently with in situ data to allow them to be used confidently for yield forecasting in an operational mode.

Greenhouse Gas Flux

The three main greenhouse gases (GHGs) emitted from agricultural sources are carbon dioxide (CO_2), methane (CH_4) and nitrous oxide (N_2O). The source of emissions (e.g., soil-based vs. animal-based) usually dictates the most appropriate measurement technique to quantify GHG emissions. Agricultural soils, which are diffuse (nonpoint) sources, can either emit or absorb CO_2 and CH_4 depending on the management practices and the environmental conditions. They are also an important source of N_2O because of the increased application of nitrogen (N) fertilizer and manure. Livestock and animal waste treatment systems are significant sources of both CH_4 and N_2O . We will briefly present examples of GHG flux measurements from agricultural sources. We will show how the combination of measurements and models is being used to improve our understanding of the interactions between management practices and GHG emissions. We will also show how the amount of GHG emissions associated with an agricultural product can help quantify the impact of a production system on the environment.

Chamber Measurements

Closed and open chambers are frequently used to quantify the impact of a change in management practices on GHG emissions from agricultural soils (Rochette et al., 1992). They are inexpensive and easy to use. Their main limitation is that they provide information on a very small area. Lessard et al. (1996; 1997) used dynamic closed chamber systems to quantify the influence of manure applications on N_2O and CH_4 emissions over a growing season. Zou et al. (2005) used chambers over rice paddies to show that there are trade-offs between CH_4 and N_2O emissions for certain management practices. For example, in contrast with continuous flooding, mid-season drainage caused a drop in CH_4 emissions, while concurrently increasing N_2O emissions. Rochette et al. (1992) showed that respiration from soil under barley was 25%

lower than from fallow (uncropped) soil and that the afternoon soil respiration averaged 22 and 17% more than morning on fallow and barley fields, respectively.

Measurements from Point Sources

Livestock operations emit a substantial amount of CH₄ from enteric fermentation and manure management. An inverse dispersion technique in conjunction with open-path instruments is ideal for measuring GHG emissions from multiple sources with large spatial and temporal variability, as is common on typical livestock operations (Flesch et al., 2005; Laubach et al., 2013). It uses a backward in time particle dispersion model which requires line-averaged concentration measurements of the gas of interest downwind and upwind of the source as well as the wind statistics provided by a sonic anemometer. Gao et al. (2011) used such a system to measure the average hourly methane emissions from a dairy feedlot for the fall and winter seasons. They showed that it is important to consider the diurnal pattern to assess the mitigation potential of a mitigation strategy. In a study on dairy farms, VanderZaag et al. (2014) showed that in the fall when the manure storage tank was full, 60% of the whole farm emissions came from the manure storage. They also reported that whole farm CH₄ emissions were 40% higher in the fall than in the spring.

Tower and Aircraft-based Flux Measurements

Tower and aircraft-based flux measurements provide useful information on GHG emissions at a wide range of scales (Pattey et al., 2006a). Ma et al. (2007) estimated the net carbon exchange, at a grassland site in California, from 2000 to 2006 using the eddy covariance technique. The net annual exchange, which varied from -88 to 141 g C m⁻² y⁻¹, depended primarily on the amount of rain during the growing period. Wagner-Riddle et al. (2007) used the flux-gradient technique to quantify the N₂O emissions associated with the spring thaw period. The flux-gradient technique is sometimes used rather than the eddy covariance technique for cases when there are no fast response sensors for the gas of interest. Over a 5 yr period in a corn-soybean-wheat rotation, they showed that N₂O emissions during November to April comprised between 30% and 90% of the annual emissions, mostly due to the large N₂O emissions during soil thawing. Pattey et al. (2006b) demonstrated the management and weather impact on N₂O fluxes during the growing season. Periods after N fertilizer applications coincided with increased N₂O fluxes. They also showed the considerable daytime variability of N₂O emissions that peaked during the midmorning and decreased in the afternoon as the soil dried. Tower-based flux measurements of N₂O have also been an excellent source of information for testing and improving biogeochemical models (Smith et al., 2002). Using the DNDC model, the climatology of N₂O emissions in Canada during spring thaw was examined by Smith et al. (2004). They estimated on average, over the seven soil groups, that the N₂O emissions during spring thaw were about 30% of the annual emissions. This information is used in Canada's national agricultural GHG inventory (Rochette et al., 2008) to scale annual emissions to account for the spring thaw period. Desjardins et al. (2010) used aircraft-based flux measurements to verify N₂O emission estimates at the regional scale. By comparing these flux measurements to process-based model estimates they were able to verify the magnitude of indirect N₂O emissions.

Process-based Models

Regardless of the temporal and spatial scales covered using various flux measurement techniques, it is clear that it is impossible to measure continuously and compare all management options. Models are then essential to fill the gap left by direct flux measurements. They help improve our understanding of the interactions between management practices and environmental conditions for a wide range of GHG sources. They also allow us to separate the environmental impacts of human activities and year to year variability due to climate. Better information on the impact of management practices is essential to improve GHG emission inventory (VanderZaag et al., 2013).

The importance of models, especially those at the farm scale are gaining prominence in tools such as HOLOS (Little et al., 2008), the “Cool Farm Tool” (Hillier et al., 2011) and ULICEES (Vergé et al., 2012). These tools are being used to provide information on the carbon footprint of agricultural products. Because of consumer demands for environmentally sustainable food production producers of agricultural products with a lower carbon footprint will likely have access to either a wider range of markets or may get a preferential treatment such as less tariffs or taxes.

Case Study: The Carbon Footprint of Beef in Canada

An on-farm model has been developed to estimate the carbon footprint of agricultural products (Vergé et al., 2012). This model was developed using GHG flux measurements obtained using the techniques described above. The cradle to farm gate carbon footprint associated with beef production in Canada was quantified using this model for each Census year from 1981 to 2006 (Desjardins et al., 2012). It was obtained by first calculating the carbon footprint of all crops in Canada (Dyer et al., 2010). Then based on the diets of cattle, we estimated the GHG emission per kg of live weight at the exit gate of the farm. We note a substantial decrease in the carbon footprint (CFb) of beef from 1981 to 2006 (Table 4.1). This is due to better breeds, better diets bigger carcass weight and improved soil management practices.

Carbon footprint estimates are very dependent on what GHG emissions are included. If we include the impact of soil carbon change in the carbon footprint (CFbc) calculation, we obtain a slightly larger carbon footprint for the period between 1981 and 1991 and a reduction in the carbon footprint for the period between 1996 and 2006. This is because of improved soil conservation practices, such as reduced tillage and reduced summer fallowing. The carbon footprint of beef also changes if the GHG emissions from cattle from the dairy sector are also included. In this case, an extra 14.4% of the GHG emissions from the dairy sector need to be allocated to meat production (IDF-FIL, 2010). The carbon footprint of all beef production in Canada including the beef from the dairy sector (CFbcd) is given in Table 6. This value is larger than the other estimates because originally all the GHG emissions from the dairy sector were associated with milk production.

This is one example of the range of carbon footprint values that can be obtained depending what is included in the calculation.

Looking Ahead

Agroclimatology is an integration of meteorological, biophysical, and hydrological parameters over spatial and temporal scales that are relevant for understanding agricultural production. This chapter discussed measurement techniques which

Table 6. Cradle to farm gate carbon footprint associated with beef production in Canada (Updated from Desjardins et al., 2012).

Year	Carbon footprint	Carbon footprint including soil carbon change	Carbon footprint including dairy sector
—kg CO ₂ e per kg LW—			
1981	16.6	16.9	18.2
1986	15.3	15.4	16.6
1991	13.7	13.9	14.9
1996	12.4	12.1	12.8
2001	10.3	9.7	10.2
2006	10.0	9.0	9.5

utilize combinations of in situ instrumentation, remote sensing instrumentation, and modeling to solve the complex interactions associated with measurements of soil moisture, crop conditions, expressions of drought, and the flux associated with greenhouse gases in agricultural landscapes.

The rapid expansion of satellite-based remote sensing technology is vastly increasing the availability of timely, inexpensive data with increasingly temporal and spatial finer resolutions. With the development and adoption of drone technology, low-level aerial observations will add even higher resolution to monitoring efforts. Scaling of data will become even more important as independent monitoring activities conducted within a field merge with more conventional coarser scale monitoring. Competitive advantages will be gained from the ability to process and interpret large data volumes with increasing timeliness for decision support.

Crowd sourced data will add complexity as to how data quality is assessed, managed, processed, and interpreted. Measurement techniques in this era of “big data” have extended beyond sensors and methodologies which derive new data from observations of the natural system to techniques that can capture the value of existing data. The measurement techniques of the future will have increasing reliance on the analytical powers of modeling, land data assimilation systems, neural network systems, and other means of optimizing the information contained in data to develop indices that better describe and measure the complex interactions of agroclimatologic processes.

References

Adams, J.R., H. McNairn, A.A. Berg, and C. Champagne. 2015. Evaluation of near-surface soil moisture data from an AAFC monitoring network in Manitoba, Canada: Implications for L-band satellite validation. *J. Hydrol.* 521:582–592. doi:10.1016/j.jhydrol.2014.10.024

Hatfield, J.L., and J.M. Baker, editors. 2005. *Micrometeorology in agricultural systems*. Agron. Monogr. 47. ASA, CSSA, and SSSA, Madison, WI.

Anderson, M.C., C.R. Hain, B.D. Wardlow, A. Pimstein, J.R. Mecikalski, and W.P. Kust. 2007. Thermal-based evaporative stress index for monitoring surface moisture depletion. In: B.D. Wardlow, M.C. Anderson, and J.P. Verdin, editors, *Remote sensing of drought: Innovative monitoring approaches*. CRC Press, Boca Raton, FL. p. 145–167.

Asner, G.P. 1998. Biophysical and biochemical sources of variability in canopy reflectance. *Remote Sens. Environ.* 64:234–253. doi:10.1016/S0034-4257(98)00014-5

Asner, G.P., C.A. Wessman, D.S. Schimel and S. Archer. 1998. Variability in leaf and litter optical properties: implications for BRDF model inversions using AVHRR, MODIS and MISR. *Remote Sens. Environ.* 63:243–257. doi:10.1016/S0034-4257(97)00138-7

- Asrar, G., R.L. Weiser, D.E. Johnson, E.T. Kanemasu, and J.M. Milleen. 1986. Distinguishing among tallgrass prairie cover types from measurements of multispectral reflectance. *Remote Sens. Environ.* 19:159–169. doi:10.1016/0034-4257(86)90069-6
- Attema, E.P.W., and F.T. Ulaby. 1978. Vegetation modelled as a water cloud. *Radio Sci.* 13:357–364. doi:10.1029/RS013i002p00357
- Baatz, R., H.R. Bogaen, H. J. Hendricks Franssen, J.A. Huisman, W. Qu, C. Montzka, and H. Vereecken. 2014. Calibration of a catchment scale cosmic-ray probe network: A comparison of three parameterization methods. *J. Hydrol.* 516:231–244. doi:10.1016/j.jhydrol.2014.02.026
- Baret, F., and G. Guyot. 1991. Potentials and limits of vegetation indices for LAI and APAR assessment. *Remote Sens. Environ.* 35:161–173. doi:10.1016/0034-4257(91)90009-U
- Baret, F., M. Weiss, D. Allard, S. Garrigues, M. Leroy, H. Jeanjean, et al. 2005. VALERI: A network of sites and a methodology for the validation of medium spatial resolution land satellite products. *Remote Sens. Environ.* 96 (1):69–89.
- Bogaen, H.R., J.A. Huisman, C. Oberdorster, and H. Vereecken. 2007. Evaluation of a low-cost soil water content sensor for wireless network applications. *J. Hydrol.* 344:32–42. doi:10.1016/j.jhydrol.2007.06.032
- Borm, L. and J.V. Zidek. 2012. Efficient stabilization of crop yield prediction in the Canadian Prairies. *Agricultural and Forest Meteorology* 152:223–232.
- Boutton, T.W., A.T. Harrison, and B.N. Smith. 1980. Distribution of biomass of species differing in photosynthetic pathway along an altitudinal gradient in southeastern Wyoming grassland. *Oecologia* 45:287–298. doi:10.1007/BF00540195
- Box, E.O., B.N. Holben, and H. Kalb. 1989. Accuracy of the AVHRR vegetation index as a predictor of biomass, primary productivity and net CO₂ flux. *Vegetatio* 80:71–89. doi:10.1007/BF00048034
- Brown, J.F., B.D. Wardlow, T. Tadesse, M.J. Hayes, and B.C. Reed. 2008. The Vegetation Drought Response Index (VegDRI): A new integrated approach for monitoring drought stress in vegetation. *GISci. Remote Sens.* 45(1):16–46. doi:10.2747/1548-1603.45.1.16
- Camacho, F., J. Cernicharo, R. Lacaze, F. Baret, and M. Weiss. 2013. GEOV1: LAI, FAPAR Essential Climate Variables and FCOVER global time series capitalizing over existing products. Part 2: Validation and intercomparison with reference products. *Remote Sens. Environ.* 137:310–329. doi:10.1016/j.rse.2013.02.030
- Ceccato, P., S. Flasse, and J.-M. Grégoire. 2002a. Designing a spectral index to estimate vegetation water content from remote sensing data: Part 2. Validation and applications. *Remote Sens. Environ.* 82:198–207. doi:10.1016/S0034-4257(02)00036-6
- Ceccato, P., N. Gobron, S. Flasse, B. Pinty, and S. Tarantola. 2002b. Designing a spectral index to estimate vegetation water content from remote sensing data: Part 1. Theoretical approach. *Remote Sens. Environ.* 82:188–197. doi:10.1016/S0034-4257(02)00037-8
- Chanasyk, D.S., and M.A. Naeth. 1996. Field measurement of soil moisture using neutron probe. *Can. J. Soil Sci.* 76:317–323. doi:10.4141/cjss96-038
- Chen, Y., and D. Or. 2006. Effects of Maxwell-Wagner polarization on soil complex dielectric permittivity under variable temperature and electrical conductivity. *Water Resour. Res.* 42:W06424. doi:10.1029/2005WR004590
- Chipanshi, A., Y. Zhang, L. Kouadio, N. Newlands, A. Davidson, H. Hill, et al. 2015. Evaluation of the Integrated Canadian Crop Yield Forecast model for in-season prediction of crop yield across the agricultural landscape. *Agric. For. Meteorol.* 206:137–150. doi:10.1016/j.agrformet.2015.03.007
- Chipanshi, A.C., Y. Zhang, N.K. Newlands, H. Hill, and D.S. Zamar. 2012. Canadian Crop Yield Forecaster (CCYF)—a GIS and statistical integration of agro-climates and remote sensing information. In: Proc. Workshop on the application of remote sensing and GIS technology on crops productivity among APEC economies, 30-31 July 2012, Asia – Pacific Economic Corporation, Beijing, People's Republic of China.
- Cosh, M.H., T.J. Jackson, R. Bindlish, J.S. Famiglietti, and D. Ryu. 2005. Calibration of an impedance probe for estimation of surface soil water content over large regions. *J. Hydrol.* 311:49–58. doi:10.1016/j.jhydrol.2005.01.003

- Cosh, M.H., T. Ochsner, J. Basara, and T.J. Jackson. 2010. The SMAP in-situ soil moisture sensor testbed: comparing in-situ sensors for satellite validation. In: Proc. IEEE International Geoscience and Remote Sensing Symposium, July 25-30, 2010. Honolulu, HI. p. 699-701. doi: 10.1109/IGARSS.2010.5652389.
- Cracknell, A.P. 2001. The exciting and totally unanticipated success of the AVHRR in applications for which it was never intended. *Adv. Space Res.* 28:233-240. doi:10.1016/S0273-1177(01)00349-0
- Davidson, A., and F. Csillag. 2001. The influence of vegetation index and spatial resolution on a two-date remote sensing derived relation to C4 species coverage. *Remote Sens. Environ.* 75:138-151. doi:10.1016/S0034-4257(00)00162-0
- de Wit, A.J.W., and C.A. van Diepen. 2007. Crop model data assimilation with the Ensemble Kalman filter for improving regional crop yield forecasts. *Agric. For. Meteorol.* 146(1-2):38-56. doi:10.1016/j.agrformet.2007.05.004
- Dean, T.J., J.P. Bell, and A.J.B. Baty. 1987. Soil moisture measurement by an improved capacitance technique, Part I. Sensor design and performance. *J. Hydrol.* 93:67-78. doi:10.1016/0022-1694(87)90194-6
- Desjardins, R.L., E. Pattey, W.N. Smith, D. Worth, B. Grant, R. Srinivasan, J.I. MacPherson, and M. Mauder. 2010. Multiscale estimates of N₂O emissions from agricultural lands. Special Issue of *Agr. Forest Meteorol.* 150(6):817-824. doi:10.1016/j.agrformet.2009.09.001
- Desjardins, R.L., D.E. Worth, X.P.C. Verge, D. Maxime, J.A. Dyer, and D. Cerkowniak. 2012. Carbon footprint of beef cattle. *Sustainability* 4:3279-3301. doi:10.3390/su4123279
- Dobriyal, P., A. Qureshi, R. Badola, and S. Ainul Hussain. 2012. A review of the methods available for estimating soil moisture and its implications for water resource management. *J. Hydrol.* 458-459:110-117. doi:10.1016/j.jhydrol.2012.06.021
- Dobson, M.C., and F.T. Ulaby. 1998. Mapping soil moisture distribution with imaging radar. In: F.M. Henderson and A.J. Lewis, editors, *Principles & applications of imaging radar*. John Wiley & Sons, New York.
- Dowd, M. 2006. A sequential Monte Carlo approach for marine ecological prediction. *Environmetrics* 17(5):435-455. doi:10.1002/env.780
- Dubois, P.C., J. Van Zyl, and T. Engman. 1995. Measuring soil moisture with imaging radars. *IEEE Trans. Geosci. Rem. Sens.* 33:4915-4926.
- Dyer, J.A., X.P.C. Vergé, R.L. Desjardins, D.E. Worth, and B.G. McConkey. 2010. The impact of increased biodiesel production on the greenhouse gas emissions from field crops in Canada. *Energy Sustain. Dev.* 14(2):73-82. doi:10.1016/j.esd.2010.03.001
- Elachi, C., and J.J. van Zyl. 2006. *Introduction to the physics and techniques of remote sensing*. Wiley, Hoboken. doi:10.1002/0471783390
- Fensholt, R., and I. Sandholt. 2005. Evaluation of MODIS and NOAA AVHRR vegetation indices with in situ measurements in a semi-arid environment. *Int. J. Remote Sens.* 26:2561-2594. doi:10.1080/01431160500033724
- Flesch, T.K., J.D. Wilson, L.A. Harper, and B.P. Crenna. 2005. Estimating gas emissions from a farm with an inverse-dispersion technique. *Atmos. Environ.* 39:4863-4874. doi:10.1016/j.atmosenv.2005.04.032
- Fourty, T., F. Baret, S. Jacquemoud, G. Schmuck, and J. Verdebout. 1996. Leaf optical properties with explicit description of its biochemical composition: direct and inverse problems. *Remote Sens. Environ.* 56:104-117. doi:10.1016/0034-4257(95)00234-0
- Franz, T.E., M. Zreda, R. Rosolem, B.K. Hornbuckle, S.L. Irvin, H. Adams, et al. 2013. Ecosystem-scale measurements of biomass water using cosmic ray neutrons. *Geophys. Res. Lett.* 40:1-5. doi:10.1002/grl.50791
- Fung, A.K., and K.S. Chen. 1992. Dependence of the surface backscattering coefficients on roughness, frequency and polarization states. *Int. J. Remote Sens.* 13:1663-1680. doi:10.1080/01431169208904219
- Gardner, W.H. 1965. Water Content. In: C.A. Black, editor, *Methods of soil analysis. Part 1. Physical and mineralogical properties, including statistics of measurement and sampling*. Amer. Soc. Agron., Soil Science Soc. of America, Madison, Wi. p. 82-127, 10.2134/agronmonogr9.1.c7.

- Garen, D.C. 1993. Revised surface water supply index for western United States. *J. Water Resour. Plan. Manage.* 119(4):437–454. doi:10.1061/(ASCE)0733-9496(1993)119:4(437)
- Gao, Z., Y. Huijun, W. Ma, J. Li, X. Liu, and R.L. Desjardins. 2011. Diurnal and seasonal patterns of methane emissions from a dairy operation in North China plain *Adv. Meteorology.* doi:10.1155/2011/190234
- Gitelson, A.A., and Y.J. Kaufman. 1998. MODIS NDVI optimization to fit the AVHRR data series: Spectral considerations. *Remote Sens. Environ.* 66:343–350. doi:10.1016/S0034-4257(98)00065-0
- Goel, N.S. 1988. Models of vegetation canopy reflectance and their use in estimation of biophysical parameters from reflectance data. *Remote Sens. Environ.* 4:1–212.
- Han, W., Z. Yang, L. Di, and R. Mueller. 2012. CropScape: A web service based application for exploring and disseminating US conterminous geospatial cropland data products for decision support. *Comput. Electron. Agric.* 84:111–123. doi:10.1016/j.compag.2012.03.005
- Hardisky, M.A., V. Klemas, and R.M. Smart. 1983. The influence of soil salinity, growth form, and leaf moisture on the spectral reflectance of spartina alterniflora species. *Photogramm. Eng. Remote Sensing* 49:77–83.
- Hastings, D.A., and W.J. Emery. 1992. The Advanced Very High Resolution Radiometer (AVHRR): A brief reference guide. *Photogramm. Eng. Remote Sensing* 58:1183–1188.
- Hatfield, J.L., G. Asrar, and E.T. Kanemasu. 1984. Intercepted photosynthetically active radiation estimated by spectral reflectance. *Remote Sens. Environ.* 14:65–75. doi:10.1016/0034-4257(84)90008-7
- Heim, R.R. 2002. A review of twentieth-century drought indices used in the United States. *Bull. Am. Meteorol. Soc.* (August):1149–1165.
- Hillier, J., C. Walter, D. Malin, T. Garcia-Suarez, L. Mila-i-Canals, and P. Smith. 2011. A farm-focused calculator for emissions from crop and livestock production. *Environ. Model. Softw.* 26(9):1070–1078. doi:10.1016/j.envsoft.2011.03.014
- Holben, B. 1986. Characteristics of maximum value composite images from temporal AVHRR data. *Int. J. Remote Sens.* 7:1417–1434. doi:10.1080/01431168608948945
- Houborg, R., M. Rodell, B. Li, R. Reichle, and B.F. Zaitchik. 2012. Drought indicators based on model assimilated GRACE terrestrial water storage observations. *Water Resour. Res.* 48:W07525. doi:10.1029/2011WR011291
- Huete, A., K. Didan, T. Miura, E.P. Rodriguez, X. Gao, and L.G. Ferreira. 2002. Overview of the radiometric and biophysical performance of the MODIS vegetation indices. *Remote Sens. Environ.* 83:195–213. doi:10.1016/S0034-4257(02)00096-2
- Huete, A.R., H.Q. Liu, K. Batchily, and W.J. van Leeuwen. 1997. A comparison of vegetation indices over a global set of TM images for EOS-MODIS. *Remote Sens. Environ.* 59:440–451. doi:10.1016/S0034-4257(96)00112-5
- Huete, A.R., and C. Justice. 1999. MODIS vegetation index (MOD13) algorithm theoretical basis document. NASA Goddard Flight Center, Greenbelt, MD. p. 129.
- Huete, A.R. 1988. A soil-adjusted vegetation index (SAVI). *Remote Sens. Environ.* 25:295–309. doi:10.1016/0034-4257(88)90106-X
- Huisman, J.A., S.S. Hubbard, J.D. Redman, and A.P. Annan. 2003. Measuring soil water content with ground penetrating radar: A review. *Vadose Zone J.* 2:476–491. doi:10.2136/vzj2003.4760
- Huisman, J.A., J.J.C. Snepvangers, W. Bouten, and G.B.M. Heuvelink. 2002. Mapping spatial variation in surface soil water content: comparison of ground-penetrating radar and time domain reflectometry. *J. Hydrol.* 269:194–207. doi:10.1016/S0022-1694(02)00239-1
- Hunt, E.R., Jr., and B.N. Rock. 1989. Detection of changes in leaf water content using Near- and Middle-Infrared reflectances. *Remote Sens. Environ.* 30:43–54. doi:10.1016/0034-4257(89)90046-1
- Hurcom, S.J., and A.R. Harrison. 1998. The NDVI and spectral decomposition for semi-arid vegetation abundance estimation. *Int. J. Remote Sens.* 19:3109–3125. doi:10.1080/014311698214217

- IDF-FIL. 2010. A common carbon footprint approach for dairy. The IDF guide to standard life cycle assessment methodology for the dairy sector. Bulletin of the International Dairy Federation. Brussels, Belgium. 45(1):46. <http://www.fil-idf.org/Public/PublicationsPage.php?ID=27121#list> (20 July 2018).
- Jackson, T.J. 2002. Passive microwave remote sensing methods. In: J.H. Dane and G.C. Topp, editors, *Methods of soil analysis: Part 4- Physical methods*. 3rd ed. SSSA. Madison, Wisconsin.
- Jackson, T.J., and C.E. Ezra. 1985. Spectral response of cotton to suddenly induced water stress. *Int. J. Biometeorol.* 6:177–185.
- Jensen, J.R. 2007. *Remote sensing of the environment: An Earth resource perspective*. Prentice Hall Upper Saddle River, NJ.
- Jiao, X., H. McNairn, J. Shang, E. Pattey, J. Liu, and C. Champagne. 2014. The sensitivity of RADARSAT-2 polarimetric SAR data to corn and soybean Leaf Area Index. *Can. J. Rem. Sens.* 37:69–81. doi:10.5589/m11-023
- Jordan, C.F. 1969. Derivation of Leaf Area Index from quality of light on the forest floor. *Ecology* 50:663–666. doi:10.2307/1936256
- Joint Research Centre. 2012. MARS crop yield forecasting system (MCYFS). European Commission. <http://www.marsop.info/marsop3/>.
- Justice, C.O., T.F. Eck, D. Tanré, and B.N. Holben. 1991. The effect of water vapour on the normalized difference vegetation index derived for the Sahelian region from NOAA AVHRR data. *Int. J. Remote Sens.* 12:1165–1187. doi:10.1080/01431169108929720
- Keyantash, J., and J.A. Dracup. 2002. The quantification of drought: An evaluation of drought indices. *Bull. Am. Meteorol. Soc.* (August):1167–1180.
- Kogan, F., N. Kussul, T. Adamenko, S. Skakun, O. Kravchenko, O. Kryvobok, A. Shelestov, A. Kolotii, O. Kussul, and A. Lavrenyuk. 2013. Winter wheat yield forecasting in Ukraine based on Earth observation, meteorological data and biophysical models. *Int. J. Appl. Earth Obs. Geoinf.* 23:192–203. doi:10.1016/j.jag.2013.01.002
- Kussul, O., N. Kussul, S. Skakun, O. Kravchenko, A. Shelestov, and A. Kolotii. 2013. Assessment of relative efficiency of using MODIS data to winter wheat yield forecasting in Ukraine. In: 2013 IEEE International Geoscience and Remote Sensing Symposium, 21–26 July 2013, Melbourne, Australia. IEEE, New York. p. 3235–3238. doi:10.1109/IGARSS.2013.6723516
- Kussul, N., A. Kolotii, S. Skakun, A. Shelestov, O. Kussul, and T. Oliynuk. 2014. Efficiency estimation of different satellite data usage for winter wheat yield forecasting in Ukraine. In: 2014 IEEE Geoscience and Remote Sensing Symposium, 13–18 July 2014, Quebec City, QC. IEEE, New York. p. 5080–5082. doi:10.1109/IGARSS.2014.6947639
- Laubach, J., M. Bai, C.S. Pinares-Patino, F.A. Phillips, T.A. Naylor, G. Molano, et al. 2013. Accuracy of micrometeorological techniques for detecting a change in methane emissions from a herd of cattle. *Agric. For. Meteorol.* 176:50–63. doi:10.1016/j.agrformet.2013.03.006
- Lessard, R., P. Rochette, E.G. Gregorich, E. Pattey, and R.L. Desjardins. 1996. N₂O fluxes from manure-amended soil under maize. *J. Environ. Qual.* 25:1371–1377. doi:10.2134/jeq1996.00472425002500060029x
- Lessard, R.L., P. Rochette, E.G. Gregorich, R.L. Desjardins, and E. Pattey. 1997. CH₄ fluxes from a soil amended with dairy cattle manure and ammonium nitrate. *Can. J. Soil Sci.* 77:179–186. doi:10.4141/S96-108
- Liaw, A., and M. Wiener. 2002. Classification and regression by random forest. *R. News.* 2(3):18–22.
- Little, S., J. Lindeman, K. Maclean, and H. Janzen. 2008. HOLOS- a tool to estimate and reduce greenhouse gases from farms. Methodology and algorithms for version 1.1.x. Agriculture and Agri-Food Canada, Ottawa, ON. Cat. No. A52-136/2008-PDF, p. 158.
- Lv, L., T.E. Franz, D.A. Robinson, and S.B. Jones. 2014. Measured and modeled soil moisture compared with cosmic-ray neutron probe estimates in a mixed forest. *Vadose Zone J.* 13(1) doi:10.2136/vzj2014.06.0077.

- Ma, S., D. Baldocchi, L. Xu, and T. Hehn. 2007. Inter-annual variability in carbon dioxide exchange of an oak/grass savanna and open grassland in California. *Agric. For. Meteorol.* 147:157–171. doi:10.1016/j.agrformet.2007.07.008
- Matile, L., R. Berger, D. Wächter, and R. Krebs. 2013. Characterization of a new heat dissipation matric potential sensor. *Sensors (Basel Switzerland)*. 13:1137–1145. doi:10.3390/s130101137
- McKee, T.B., N.J. Doesken, and J. Kleist. 1993. The relationship of drought frequency and duration to time scales. In: *Proc. Eighth Conf. on Applied Climatology*, Anaheim, CA. 17–22 Jan. 1993. Amer. Meteorol. Soc., Washington, D.C. p. 179–184.
- McNairn, H., T.J. Jackson, G. Wiseman, S. Bélair, A. Berg, P.R. Bullock, et al. 2015. The soil moisture active passive validation experiment 2012 (SMAPVEX12): Pre-launch calibration and validation of the SMAP satellite. *IEEE Trans. Geosci. Rem. Sens.* 53:2784–2801. doi:10.1109/TGRS.2014.2364913
- Meisami-asl, E., A. Sharifi, H. Mobli, A. Eyvani, and R. Alimardani. 2012. On-site measurement of soil moisture content using an acoustic system. *Agric. Eng. Int. CIGR J.* 15(4):1–8 <http://www.cigrjournal.org>.
- Meng, L., and S.M. Quiring. 2008. A comparison of soil moisture models using soil climate analysis network observations. *J. Hydrometeorol.* 9:641–659. doi:10.1175/2008JHM916.1
- Merzouki, A., H. McNairn, and A. Pacheco. 2011. Mapping soil moisture using RADAR-SAT-2 data and local autocorrelation statistics. *IEEE J. Sel. Top. Appl. Earth Obs. Remote Sens.* 4:128–137. doi:10.1109/JSTARS.2011.2116769
- Merzouki, A., and H. McNairn. 2015. Toward operational use of Synthetic Aperture Radar (SAR) for surface soil moisture monitoring for agriculture: Preparing for the RADAR-SAT Constellation Mission. *Can. J. Rem. Sens.*
- Mkhabela, M.S., P. Bullock, S. Raj, S. Wang, and Y. Yang. 2011. Crop yield forecasting on the Canadian Prairies using MODIS NDVI data. *Agric. For. Meteorol.* 151:385–393. doi:10.1016/j.agrformet.2010.11.012
- Mladenova, I.E., T.J. Jackson, E. Njoku, R. Bindlish, S. Chan, M.H. Cosh, et al. 2014. Remote monitoring of soil moisture using passive microwave-based techniques—Theoretical basis and overview of selected algorithms for AMSR-E. *Remote Sens. Environ.* 144:197–213. doi:10.1016/j.rse.2014.01.013
- Morissette, J.T., F. Baret, J.L. Privette, R.B. Myneni, J.E. Nickeson, S. Garrigues, et al. 2006. Validation of global moderate-resolution LAI products: A framework proposed within the CEOS land product validation subgroup. *IEEE Trans. Geosci. Rem. Sens.* 44(7):1804–1817. doi:10.1109/TGRS.2006.872529
- Myneni, R.B., J. Ross, and G. Asrar. 1989. A review on the theory of photon transport in leaf canopies. *Agric. For. Meteorol.* 45:1–153. doi:10.1016/0168-1923(89)90002-6
- Myneni, R.B., S. Hoffman, Y. Knyazikhin, J.L. Privette, J. Glassy, Y. Tian, Y. Wang, X. Song, Y. Zhang, and G.R. Smith. 2002. Global products of vegetation leaf area and fraction absorbed PAR from year one of MODIS data. *Remote Sens. Environ.* 83:214–231. doi:10.1016/S0034-4257(02)00074-3
- Myneni, R.B., R. Ramakrishna, R.R. Nemani, and S.W. Running. 1997. Estimation of global leaf area index and absorbed PAR using radiative transfer models. *IEEE Trans. Geosci. Rem. Sens.* 35:1380–1393. doi:10.1109/36.649788
- Newlands, N., D. Zamar, A.L. Kouadio, Y. Zhang, A. Chipanshi, A. Potgieter, S. Toure, and H. Hill. 2014. An integrated, probabilistic model for improved seasonal forecasting of agricultural crop yield under environmental uncertainty. *Front. Environ. Sci* 2:17. doi:10.3389/fenvs.2014.00017
- Nghiem, S.V., B.D. Wardlow, D. Allured, M.D. Svoboda, D. LeComte, M. Rosencrans, S.K. Chan and G. Neumann. 2012. Microwave remote sensing of soil moisture: Science and applications. In: B.D. Wardlow, M.C. Anderson, and J.P. Verdin, editors, *Remote sensing of drought: Innovative monitoring approaches*. CRC Press, Boca Raton, FL. p. 197–226.
- Nikolova, S., S. Bruce, L. Randall, G. Barrett, K. Ritman, and M. Nicholson. 2012. Using remote sensing data and crop modeling to improve production forecasting: A scoping study. Technical Report 12.3. Department of Agriculture, Fisheries and Forestry,

- Australian Bureau of Agricultural and Resource Economics and Sciences (ABARES), Australian Government, Canberra, Australia.
- NOAA Drought Task Force. M. Hoerling, Lead; S. Schubert and K. Mo, Co-Leads. 2013. An interpretation of the origins of the 2012 Central Great Plains drought. NOAA National Integrated Drought Information System, Washington, D.C. www.drought.gov/drought/content/resources/reports (Accessed 16 July 2019).
- Oh, Y., K. Sarabandi, and F.T. Ulaby. 1992. An empirical model and an inversion technique for radar scattering from bare soil surfaces. *IEEE Trans. Geosci. Rem. Sens.* 30:370–381. doi:10.1109/36.134086
- Ojo, E.R., P.R. Bullock, J. L'Heureux, J. Powers, H. McNairn and A. Pacheco. 2015. Calibration and evaluation of a frequency domain reflectometry sensor for the real-time in-situ monitoring. *Vadose Zone J.* 14 (3) doi:10.2136/vzj2014.08.0114.
- Otkin, J.A., M.C. Anderson, C. Hain, and M. Svoboda. 2014. Examining the relationship between drought development and rapid changes in the evaporative stress index. *J. Hydrometeorol.* 15:938–956. doi:10.1175/JHM-D-13-0110.1
- Otkin, J.A., M.C. Anderson, C. Hain, and M. Svoboda. 2015. Using temporal changes in drought indices to generate probabilistic drought intensification forecasts. *J. Hydrometeorol.* 16:88–105. doi:10.1175/JHM-D-14-0064.1
- Otkin, J.A., M.C. Anderson, C. Hain, I. Mladenova, J. Basara, and M. Svoboda. 2013. Examining rapid onset drought development using the thermal infrared-based evaporative stress index. *J. Hydrometeorol.* 14:1057–1074. doi:10.1175/JHM-D-12-0144.1
- Pacheco, A., H. McNairn, A. Mahmoodi, C. Champagne, and Y. Kerr. 2015. The impact of national land cover and soils data on soil moisture and ocean salinity (SMOS) soil moisture retrieval over Canadian agricultural landscapes. *IEEE J. Sel. Top. Appl. Earth Obs. Remote Sens.* doi:10.1109/JSTARS.2015.2417832
- Palmer, W.C. 1965. Meteorological drought. U.S. Weather Bureau Research Paper 45, U.S. Department of Commerce, Washington, D.C.
- Paltridge, G.W., and J. Barber. 1988. Monitoring grassland dryness and fire potential in Australia with NOAA/AVHRR data. *Remote Sens. Environ.* 25:381–394. doi:10.1016/0034-4257(88)90110-1
- Pattey, E., G. Edwards, I.B. Strachan, R.L. Desjardins, S. Kaharabata, and C. Wagner Riddle. 2006a. Towards standards for measuring greenhouse gas flux from agricultural fields using instrumented towers. *Can. J. Soil Sci.* 86:373–400. doi:10.4141/S05-100
- Pattey, E., I.B. Strachan, R.L. Desjardins, G.C. Edwards, D. Dow, and I.J. MacPherson. 2006b. Application of a tunable diode laser to the measurement of CH₄ and N₂O fluxes from field to landscape scale using several micrometeorological techniques. *Agric. For. Meteorol.* 136:222–236. doi:10.1016/j.agrformet.2004.12.009
- Peñuelas, J., and Y. Inoue. 1999. Reflectance indices indicative of changes in water and pigment contents of peanut and wheat leaves. *Photosynthetica* 36:355–360. doi:10.1023/A:1007033503276
- Petropoulos, G.P. 2014. Remote sensing of energy fluxes and soil moisture Content. CRC Press, Taylor and Francis Group, Boca Raton, FL.
- Potgieter, A.B., G.L. Hammer and A. Doherty. 2006. Oz-Wheat: A regional-scale crop yield simulation model for Australian wheat. Information Series. Queensland Department of Primary Industries & Fisheries, Brisbane, Australia. p. 20.
- Prince, S.D. 1991. A model of regional primary production for use with coarse resolution satellite data. *Int. J. Remote Sens.* 6:1313–1330. doi:10.1080/01431169108929728
- Purevdorj, T., R. Tateishi, T. Ishiyama, and Y. Honda. 1998. Relationships between percent vegetation cover and vegetation indices. *Int. J. Remote Sens.* 19:3519–3535. doi:10.1080/014311698213795
- Qian, B., R. De Jong, R. Warren, A. Chipanshi, and H. Hill. 2009. Statistical spring wheat yield forecasting for the Canadian Prairie provinces. *Agric. For. Meteorol.* 149:1022–1031. doi:10.1016/j.agrformet.2008.12.006
- Reichert, G.C., and D. Caissy. 2002. A reliable crop condition assessment program (CCAP) incorporating NOAA AVHRR data, a geographical information system, and the

- internet. Statistics Canada. Ottawa, ON. <http://www26.statcan.ca/ccap-peec/esri-2002conf-eng.jsp> (verified 20 July 2018).
- Robinson, D.A., S.B. Jones, J.M. Wraith, D. Or, and S.P. Friedman. 2003. A review of advances in dielectric and electrical conductivity measurement in soils using Time Domain Reflectometry. *Vadose Zone J.* 2:444–475. doi:10.2136/vzj2003.4440
- Robock, A., K.Y. Vinnikov, G. Srinivasan, J.K. Entin, S.E. Hollinger, N.A. Speranskaya, and A. Namkhai. 2000. The global soil moisture data bank. *Bull. Am. Meteorol. Soc.* 81:1281–1299. doi:10.1175/1520-0477(2000)081<1281:TGSMDB>2.3.CO;2
- Rochette, P., E.G. Gregorich, and R.L. Desjardins. 1992. Comparison of static and dynamic closed chambers for measurement of soil respiration under field conditions. *Can. J. Soil Sci.* 72:605–609. doi:10.4141/cjss92-050
- Rochette, P., D. Worth, E. Huffman, J.A. Brierley, B.G. McConkey, J.Y. Yang, J.J. Hutchinson, R.L. Desjardins, R. Lemke, and S. Gameda. 2008. Inventory of agricultural N₂O emissions in Canada using a country-specific methodology. *Can. J. Soil Sci.* 88(5):655–669. doi:10.4141/CJSS07026
- Ross, J.K. 1981. *The radiation regime and architecture of plant stands.* Kluwer Boston. Hingham, MA doi:10.1007/978-94-009-8647-3
- Romano, N. 2014. Soil moisture at local scale: Measurements and simulations. *J. Hydrol.* 516:6–20. doi:10.1016/j.jhydrol.2014.01.026
- Rouse, J.W., R.H. Haas, J.A. Schell, and D.W. Deering. 1973. Monitoring vegetation systems in the Great Plains with ERTS-1. *Proceedings of the Third Earth Resources Technology Satellite Symposium*, 10-14 Dec. 1973. Goddard, MD. NASA, Washington, D.C. p. 309-317.
- Running, S.W., R.R. Nemani, D.L. Peterson, L.E. Band, D.F. Potts, L.L. Pierce, and M.A. Spanner. 1989. Mapping regional evapotranspiration and photosynthesis by coupling satellite data with ecosystem simulation. *Ecology* 70:1090–1101. doi:10.2307/1941378
- Schaefer, G.L., M.H. Cosh, and T.J. Jackson. 2007. The USDA natural resources conservation service Soil Climate Analysis Network (SCAN). *J. Atmos. Ocean. Technol.* 24:2073–2077. doi:10.1175/2007JTECHA930.1
- Schmugge, T., T.J. Jackson, and H.L. McKim. 1980. Survey of methods for soil moisture determination. *Water Resour. Res.* 16(6):961–979. doi:10.1029/WR016i006p00961
- Sellers, P.J. 1985. Canopy reflectance, photosynthesis and transpiration. *Int. J. Remote Sens.* 6:1335–1372. doi:10.1080/01431168508948283
- Semenov, M., and F.J. Doblas-Reyes. 2007. Utility of dynamical seasonal forecasts in predicting crop yield. *Clim. Res.* 34:71–81. doi:10.3354/cr034071
- Seyfried, M.S., L.E. Grant, E. Du, and K. Humes. 2005. Dielectric loss and calibration of the hydra probe soil water sensor. *Vadose Zone J.* 4:1070–1079. doi:10.2136/vzj2004.0148
- Shafer, B.A., and L.E. Dezman. 1982. Development of a surface water supply index (SWSI) to assess the severity of drought conditions in snowpack runoff areas. In: *Proceedings of the 50th Annual Western Snow Conference*, Reno, NV. Western Snow Conference, Brush Prairie, WA. p. 164-175.
- Smith, W.N., R.L. Desjardins, B. Grant, C. Li, M. Corre, P. Rochette, and R. Lemke. 2002. Testing the DNDC model using N₂O emissions at two experimental sites. *Can. J. Soil Sci.* 82:365–374. doi:10.4141/S01-048
- Smith, W.N., B. Grant, R.L. Desjardins, R. Lemke, and C. Li. 2004. Estimates of the inter-annual variations of N₂O emissions from agricultural soils in Canada. *Nutr. Cycl. Agroecosyst.* 68:37–45. doi:10.1023/B:FRES.0000012230.40684.c2
- Statistics Canada. 2012. *Definitions, data sources and methods of Field Crop Reporting Series.* Record number: 3401. Agriculture Division, Statistics Canada, Ottawa, ON. <http://www.statcan.gc.ca/imdb-bmdi/3401-eng.htm> (verified 20 July 2018).
- Stenitzer, E. 1993. Monitoring soil moisture regime of field crops with gypsum blocks. *Theor. Appl. Climatol.* 48:159–165. doi:10.1007/BF00864922
- Svoboda, M., D. LeComte, M. Hayes, R. Heim, K. Gleason, J. Angel, et al. 2002. The drought monitor. *Bull. Am. Meteorol. Soc.* 83:1181–1190. doi:10.1175/1520-0477(2002)083<1181:TDM>2.3.CO;2

- Topp, G.C., J.L. Davis, A.P. Annan. 1980. Electromagnetic determination of soil water: Measurements in coaxial transmission lines. *Water Resour. Res.* 16:574–582. doi:10.1029/WR016i003p00574
- Tran, A.P., P. Bogaert, F. Wiaux, M. Vanclooster, and S. Lambot. 2015. High-resolution space-time quantification of soil moisture along a hillslope using joint analysis of ground penetrating radar and frequency domain reflectometry data. *J. Hydrol.* 523:252–261. doi:10.1016/j.jhydrol.2015.01.065
- Trishchenko, A.P., J. Cihlar, and Z. Li. 2002. Effects of spectral response function on surface reflectance and NDVI measured with moderate resolution satellite sensors. *Remote Sens. Environ.* 81:1–18. doi:10.1016/S0034-4257(01)00328-5
- Tucker, C.J. 1979. Red and photographic infrared linear combinations for monitoring vegetation. *Remote Sens. Environ.* 8:127–150. doi:10.1016/0034-4257(79)90013-0
- Tucker, C.J., I.Y. Fung, C.D. Keeling, and R.H. Gammon. 1986. Relationship between atmospheric CO₂ variations and satellite-derived vegetation index. *Nature* 319:195–199. doi:10.1038/319195a0
- Tucker, C.J., W.W. Newcomb, S.O. Los, and S.D. Prince. 1991. Mean and inter-year variation of growing-season normalized difference vegetation index for the Sahel 1981–1989. *Int. J. Remote Sens.* 12:1133–1135. doi:10.1080/01431169108929717
- Ulaby, F.T., R.K. Moore, and A.K. Fung. 1986. *Microwave remote sensing: Active and passive*. Vol. III. From theory to applications. Artech House, Dedham, MA.
- VanderZaag, A.C., J.D. MacDonald, L. Evans, X.P.C. Verge, and R.L. Desjardins. 2013. Towards an inventory of methane emissions from manure management that is responsive to changes on Canadian farms. *Environ. Res. Lett.* 8(3):035008. doi:10.1088/1748-9326/8/3/035008
- VanderZaag, A.C., T.K. Flesch, R.L. Desjardins, H. Baldé, and T. Wright. 2014. Methane emissions from two dairy farms in eastern Ontario: Seasonal and manure-management effects. *Agric. For. Meteorol.* 194:259–267. doi:10.1016/j.agrformet.2014.02.003
- Vergé, X.P.C., J.A. Dyer, D.E. Worth, W.N. Smith, R.L. Desjardins, and B.G. McConkey. 2012. A greenhouse gas and soil carbon model for estimating the carbon footprint of livestock production in Canada. *Animals (Basel)* 2:437–454. doi:10.3390/ani2030437
- Vermote, E.F., and N.Z. Saleous. 2006. Calibration of NOAA16 AVHRR over a desert site using MODIS data. *Remote Sens. Environ.* 105:214–220. doi:10.1016/j.rse.2006.06.015
- Vicente-Serrano, S.M., B. Santiago, J. Lorenzo-Lacruz, J.J. Camarero, J.I. López-Moreno, C. Azorin-Molina, et al. 2012. Performance of drought indices for ecological, agricultural, and hydrological applications. *Earth Interactions.* 16(10):1–27. <http://EarthInteractions.org>
- Wagner-Riddle, C., A. Furon, N.L. McLaughlin, I. Lee, J. Barbeau, S. Jayasundara, et al. 2007. Intensive measurement of nitrous oxide emissions from a corn-soybean-wheat rotation under two contrasting management systems over 5 years. *Glob. Change Biol.* 13:1722–1736. doi:10.1111/j.1365-2486.2007.01388.x
- Weiser, R.L., G. Asrar, G.P. Miller, and E.T. Kanemasu. 1986. Assessing grassland biophysical characteristics from spectral measurements. *Remote Sens. Environ.* 20:141–152. doi:10.1016/0034-4257(86)90019-2
- Willite, D.A., and M.H. Glanz. 1985. Understanding the drought phenomenon: The role of definitions. *Water Int.* 10:111–120. doi:10.1080/02508068508686328
- World Meteorological Organization. 2012. Standardized precipitation index user guide. WMO-No. 1090. World Meteorological Organization (WMO), Geneva, Switzerland. http://www.wamis.org/agm/pubs/SPI/WMO_1090_EN.pdf (verified 20 July 2018).
- World Meteorological Organization. 2008. Guide to meteorological instruments and methods of observation WMO-No. 8. World Meteorological Organization (WMO), Geneva, Switzerland. <https://www.wmo.int/pages/prog/www/IMOP/CIMO-Guide.html> (verified 20 July 2018).
- Wu, B., J. Meng, Q. Li, N. Yan, X. Du, and M. Zhang. 2014. Remote sensing-based global crop monitoring: Experiences with China's CropWatch system. *Int. J. Digit. Earth* 7(2):113–137. doi:10.1080/17538947.2013.821185

- Zaitchik, B.F., M. Rodell, and R.H. Reichle. 2008. Assimilation of GRACE terrestrial water storage into a land surface model: Results for the Mississippi River basin. *J. Hydrometeorol.* 9:535–548. doi:10.1175/2007JHM951.1
- Zou, J., Y. Huang, J. Jiang, X. Zhang and R.L. Sass. 2005. A 3-year field measurement of methane and nitrous oxide emissions from rice paddies in China: Effects of water regime, crop residue, and fertilizer application. *Global Biogeochemical Cycles.* 19(2):GB2021. doi:10.29/2004GB002401.
- Zreda, M., D. Desilets, T.P.A. Ferre', and R.L. Scott. 2008. Measuring soil moisture content non-invasively at intermediate spatial scale using cosmic-ray neutrons. *Geophys. Res. Lett.* 35:L21402. doi:10.1029/2008GL035655
- Zreda, M., W.J. Shuttleworth, X. Zeng, C. Zweck, D. Desilets, T. Franz, and R. Rosolem. 2012. COSMOS: The cosmic-ray soil moisture observing system. *Hydrol. Earth Syst. Sci.* 16:4079–4099. doi:10.5194/hess-16-4079-2012